Hindawi
Advances in Materials Science and Engineering
Volume 2017, Article ID 6590606, 8 pages
https://doi.org/10.1155/2017/6590606

Research Article

Computation of Heterojunction Parameters at Low Temperatures in Heterojunctions Comprised of n-Type β-$FeSi_2$ Thin Films and p-Type Si(111) Substrates Grown by Radio Frequency Magnetron Sputtering

Phongsaphak Sittimart, Adison Nopparuchikun, and Nathaporn Promros

Department of Physics, Faculty of Science, King Mongkut's Institute of Technology Ladkrabang, Bangkok 10520, Thailand

Correspondence should be addressed to Nathaporn Promros; nathaporn_promros@kyudai.jp

Received 17 October 2016; Revised 2 January 2017; Accepted 29 January 2017; Published 2 March 2017

Academic Editor: Mikhael Bechelany

In this study, n-type β-$FeSi_2$/p-type Si heterojunctions, inside which n-type β-$FeSi_2$ films were epitaxially grown on p-type Si(111) substrates, were created using radio frequency magnetron sputtering at a substrate temperature of 560°C and Ar pressure of 2.66×10^{-1} Pa. The heterojunctions were measured for forward and reverse dark current density-voltage curves as a function of temperature ranging from 300 down to 20 K for computation of heterojunction parameters using the thermionic emission (TE) theory and Cheung's and Norde's methods. Computation using the TE theory showed that the values of ideality factor (n) were 1.71 at 300 K and 16.83 at 20 K, while the barrier height (ϕ_b) values were 0.59 eV at 300 K and 0.06 eV at 20 K. Both of the n and ϕ_b values computed using the TE theory were in agreement with those computed using Cheung's and Norde's methods. The values of series resistance (R_s) computed at 300 K and 20 K by Norde's method were 10.93 Ω and 0.15 MΩ, respectively, which agreed with the R_s values found through computation by Cheung's method. The dramatic increment of R_s value at low temperatures was likely attributable to the increment of n value at low temperatures.

1. Introduction

At present, semiconducting iron disiliside (β-$FeSi_2$) has received much attention for utilization in novel low-cost optoelectronic devices in part due to its various attractive physical properties [1–3]. It has been reported that β-$FeSi_2$ can be epitaxially grown on Si with 2–5% lattice mismatches [4]. Furthermore, its composition consists of nontoxic elements (Fe and Si) [5]. More importantly, it possesses high optical absorption coefficients (greater than 10^5 cm^{-1} at photon energies above 1.5 eV) [6, 7] and a direct band gap of 0.85 eV corresponding to an optical telecommunication wavelength in the spectral range of near-infrared (NIR) [8, 9].

Molecular beam epitaxy [10], ion beam synthesis [11], and reactive deposition epitaxy [12] have previously been utilized for growth of β-$FeSi_2$ thin films. In order to grow β-$FeSi_2$, these methods require a postannealing procedure at temperatures of at least 800°C [13]. Since the annealing procedure accelerates the diffusion of Fe atoms into the Si side, it is a potential cause for fabricated heterojunctions without rectifying action. Consequently, there is the occurrence of deep trap levels in the Si, which could act as leakage centers for the rectifying action [14]. Hence, the growth of β-$FeSi_2$ thin films at low temperatures is preferable. Previously, the authors utilized radio frequency magnetron sputtering (RFMS) for the growth of β-$FeSi_2$ at low argon (Ar) pressure [15]. Such low-pressure sputtering is effective for suppressing the diffused Fe atoms to the Si, whereas enhancing the kinetic energy of the grown species as the increased means free path is effective for β-$FeSi_2$ film growth at low temperatures. The authors confirmed that the β-$FeSi_2$ thin films grown by RFMS were epitaxially grown on p-type Si(111) substrates at a substrate temperature of 560°C. Furthermore, the n-type β-$FeSi_2$/p-type Si heterojunctions were fabricated and

subsequently utilized as NIR photodiodes. Their photodetection properties exhibited obvious improvement at low temperatures.

As such, the aim of the present study was to further investigate the electrical characteristics of n-type β-$FeSi_2$/p-type Si heterojunctions grown using RFMS. Their forward and reverse dark current density-voltage (J-V) curves were measured as a function of temperature ranging from 300 down to 20 K. The values for heterojunction parameters such as ideality factor (n), barrier height (ϕ_b), and saturation current density (J_0) including the series resistance (R_s) were computed using the thermionic emission (TE) theory and Cheung's and Norde's methods. Based on the totality of knowledge among the group members, this manuscript represents the first investigation of its kind for heterojunction parameters at low temperatures for n-type β-$FeSi_2$/p-type Si heterojunctions grown by RFMS using the aforementioned theory and methods.

2. Materials and Methods

β-$FeSi_2$ layers were grown on Si(111) substrates by using $FeSi_2$ alloy targets. Before the growth of β-$FeSi_2$ layers, the native oxide layer on the Si substrates was eliminated by immersion of the substrates in a diluted hydrofluoric acid (HF) solution and rinsing in deionized water. After cleaning, the Si substrates were immediately introduced to the inside of an RFMS system. The pressure inside the chamber was evacuated down to less than 10^{-4} Pa. β-$FeSi_2$ layers with a thickness of 300 nm were grown on p-type Si(111) substrates at a substrate temperature of 560°C for 10 hours. The sputtering pressure was maintained at 2.66×10^{-1} Pa under Ar atmosphere, with RF power of 20 W tuned by using an RF automatching system performed for the discharge of Ar gas. In order to form front and back electrodes at room temperature after the growth of the β-$FeSi_2$ layers on Si substrates, Pd and Al were grown using another RFMS system on the front Si substrate in a finger-shaped formation and on the entire back of the β-$FeSi_2$ layer, respectively.

The crystallinity for the β-$FeSi_2$ thin films was studied using X-ray diffraction (XRD; Rigaku RINT-2000/PC), while the surface morphology was investigated by Scanning Electron Microscope (SEM: Hitachi S-4700 Scanning Electron Microscope). The dark J-V curves as a function of temperature ranging from 300 down to 20 K for the present heterojunctions were measured under forward and reverse bias conditions by using a source meter (Keithley 2400). The thermionic emission (TE) theory and Cheung's and Norde's methods were utilized for computation of the heterojunction parameters, including the values of n, ϕ_b, J_0, and R_s. To evaluate the heterojunction parameters by TE theory, the n value was computed from the slope of the linear part obtained from the plot of $\ln J$ versus V, while the ϕ_b value was computed from the J_0 value computed from the straight line intercept of the $\ln J$-V at an applied bias voltage of 0 V. In addition, the group was made aware of the fact that the value of J_0 for activation energy (E_a) could be computed from the slope of the Arrhenius plot of $\ln J_0$ versus $1000/T$. To evaluate the R_s value by Cheung's method, the relationships of $dV/d(\ln J)$-J and Cheung's function ($H(J)$) [16–18] and J were plotted. Subsequently, the value for R_s was computed from the slope of these plots. To affirm the agreement and precision of the values for ϕ_b and R_s, Norde's method was utilized, by which the relationship between Norde's function ($F(V)$) [16, 17, 19] and V was plotted to compute ϕ_b as well as R_s from the minimum point of $F(V)$-V plot.

3. Results and Discussion

The XRD diffraction pattern for β-$FeSi_2$ thin films grown using RFMS on Si(111) substrates at a substrate temperature of 560°C and Ar pressure of 2.66×10^{-1} Pa is illustrated in Figure 1(a). The XRD pattern demonstrates a weak 404/440 diffraction peak as well as a strong 202/220 diffraction peak. These observed peaks are typical for epitaxial growth of β-$FeSi_2$ thin films on Si(111) substrates. Figure 1(b) shows a pole figure pattern for the β-440/404 peak. The grown β-$FeSi_2$ films demonstrate the appearance of three epitaxial variants that are rotated by an angle of 120° with respect to each other.

Figure 2(a) displays an SEM micrograph for the surface of the β-$FeSi_2$ thin films grown by RFMS on Si(111) substrates. It is clear that the β-$FeSi_2$ thin films consist of a large amount of crystallites on the small side. Figure 2(b) illustrates a cross-sectional SEM micrograph of the β-$FeSi_2$ thin films, which clearly exhibited a sharp interface between the Si substrates and β-$FeSi_2$ thin films. Furthermore, the grown β-$FeSi_2$ thin films were uniform.

The J-V curves for the n-type β-$FeSi_2$/p-type Si heterojunctions grown by RFMS on a logarithmic scale as a function of temperature ranging from 300 down to 20 K under forward and reverse bias conditions in the applied bias voltage range of −1.5 to +1.5 V are displayed in Figure 3. All of the measurements were carried out in the dark. From particular consideration at room temperature, the fabricated heterojunctions exhibited a clear rectifying action similar to conventional p-n abrupt heterojunctions, which is due to the successful formation of a junction between β-$FeSi_2$ thin films and Si substrates using RFMS at a substrate temperature of 560°C. Furthermore, this rectifying action evidently improved at lower temperatures. However, the β-$FeSi_2$/Si heterojunctions had a large leakage current at room temperature, which is likely because of the partially diffused Fe atoms in the depletion region of the Si sides acting as leakage centers for the carriers. This leakage current diminished at low temperatures as well. In addition, the J-V curves also showed linearity variation in a large voltage range, limited by the R_s effect at a high forward applied bias voltage. From consideration of the region of applied forward bias voltage $\leq$ 0.2 V, the forward current density exhibited a linear change with the applied bias voltage across the heterojunction. This can be described by means of the TE theory as the following relationship [20–23]:

$$J = J_0 \left[\exp\left(\frac{qV}{nkT} \right) - 1 \right], \quad (1)$$

where V is the applied bias voltage across the heterojunction, J is the current density, T is the absolute temperature, k is Boltzmann's constant, q is the electron charge, n is

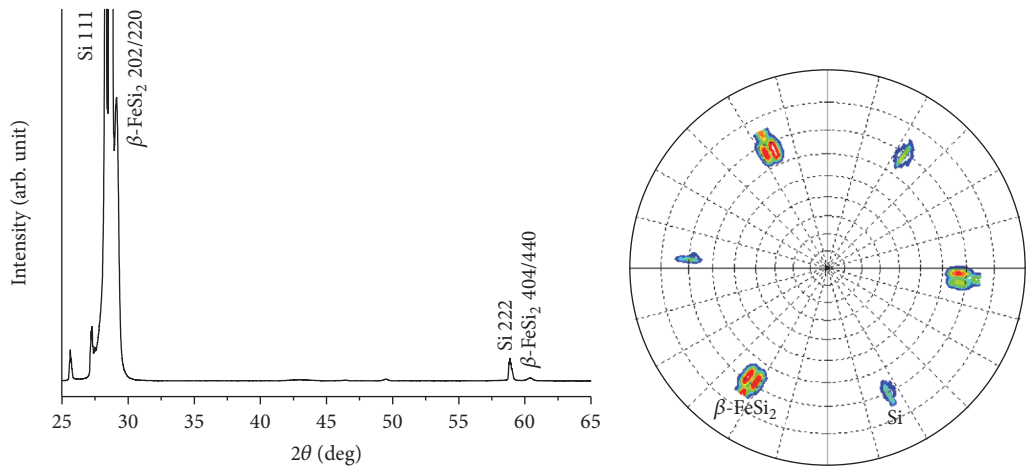

Figure 1: (a) 2θ-θ XRD pattern for β-$FeSi_2$ thin films grown on Si(111) substrates and (b) a pole figure pattern for the β-440/404 diffraction peak.

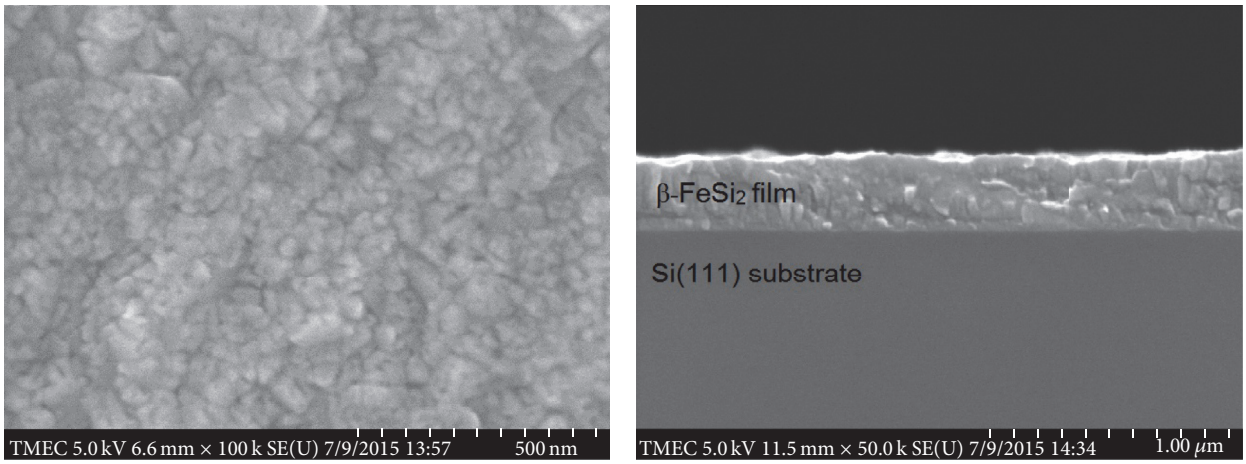

Figure 2: (a) SEM micrograph of the surface for β-$FeSi_2$ thin films grown by RFMS on Si(111) substrates and (b) a cross-sectional SEM micrograph of the β-$FeSi_2$ thin films on Si(111) substrate.

the heterojunction ideality factor, and J_0 is the saturation current density, which can be computed from the straight line intercept of the y-axis of ln J-V at an applied bias voltage of 0 V. After the value for J_0 is computed, the ϕ_b value can be computed by the following equation:

$$J_0 = A^* T^2 \exp\left(\frac{-q\phi_b}{kT}\right). \quad (2)$$

Based on (1) for the V value higher than $3kT/q$, the n value can be computed from the slope of the linear part of ln J-V as the following equation:

$$n = \frac{q}{kT}\frac{dV}{d(\ln J)} = \frac{q}{kT}\frac{1}{\text{slope}}. \quad (3)$$

Estimation of the n value following (3) can indicate the characteristics of the rectifying behavior in a junction. If it equals unity, the junction is ideal. Conversely, the junction is flawed if the value of n increases. In the case of the n value being equal to one, the transportation mechanism across the junction of the carrier is governed by a thermal diffusion process. If the n value is greater than one and lower than or equal to two, the transportation mechanism across the junction of the carrier is dominated by a generation-recombination (G-R) process. Besides, the transportation mechanism of the carrier is probably governed by a carrier tunneling process if the n value is greater than two [22].

Figure 4 illustrates a plot of n value versus the temperature for the present heterojunctions. By computation using (3), the n value at 300 K was 1.71 and remained nearly constant at a temperature ranging from 300 down to 120 K. As mentioned above, an n value greater than one and lower than two was suggestive of the transportation mechanism across the junction of the carrier being governed by a G-R process at the

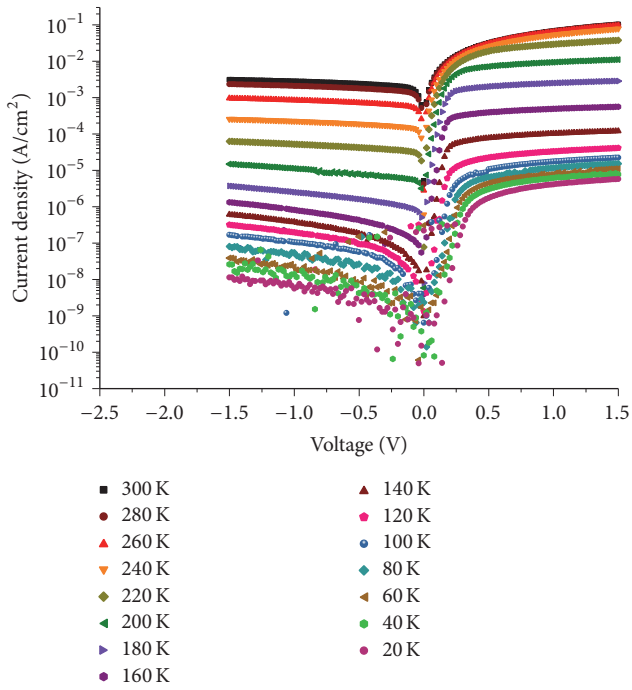

Figure 3: Semilogarithmic plot of the dark *J-V* curves of the present heterojunctions under forward and reverse bias conditions in the voltage range of −1.5 to +1.5 V at temperatures from 300 down to 20 K.

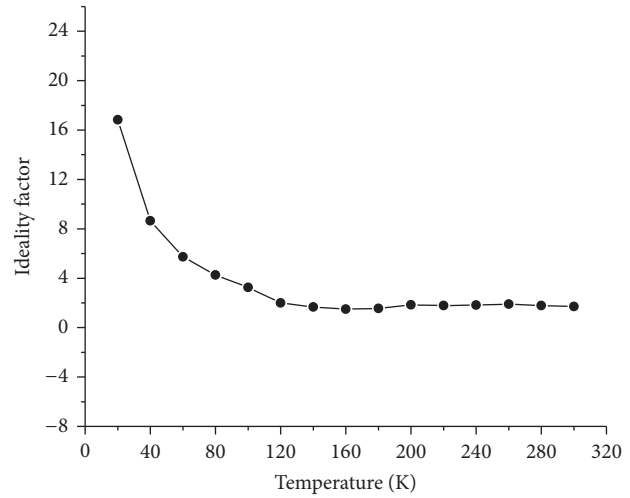

Figure 4: Plot of the *n* value versus temperature.

β-$FeSi_2$/Si heterojunction interface [24]. The existing defects in the β-$FeSi_2$ layer might create deep energy levels in the bandgap, which could behave as recombination centers. At a temperature of 100 K, the *n* value was computed at 3.25 and increased to 16.83 at 20 K. When the *n* value was higher than two, the suggestion is that the transportation mechanism across the junction of the carrier in this range of temperature was governed by a tunneling process [24]. This is likely due to the existing interface states at the interface of the β-$FeSi_2$/Si heterojunctions. The heterojunctions possess a large value for *n*, which is likely owing to the presence of a flawed contact behavior as well as the result of inhomogeneity and tunneling [25]. When the values of J_0 become known, the value for activation energy (E_a) can be computed by the following relation [21, 22, 26]:

$$J_0 \propto \exp\left(\frac{\Delta E_a}{kT}\right). \tag{4}$$

Figure 5 illustrates an Arrhenius plot for $\ln J_0$ versus $1000/T$. From the plot, the J_0 value was 5.34×10^{-4} A/cm^2 at room temperature and decreased to 9.93×10^{-12} A/cm^2 at 20 K. The two regions indicate that there are two values for E_a in the present heterojunctions. The slopes for each region can compute the values of E_a. At 120–300 K, the recombination process is dominant with an E_a value of 0.24 eV, whereas the carrier tunneling process is dominant with an E_a value of 9.18 meV in temperatures below 120 K.

After the computation of the J_0 value, the ϕ_b value can be computed using (2). The inset of Figure 5 shows the plot of ϕ_b versus temperature. At room temperature, the ϕ_b value was 0.59 eV. This value decreased to 0.06 eV at 20 K. From the experimental results, the value of *n* increased and the value of ϕ_b decreased at low temperatures. This is likely because of barrier height inhomogeneity, which may be attributable to the variation in thickness and composition of the interfacial layer as well as nonuniformity of the interfacial charges [27, 28].

There are many methods to acquire the value of R_s. For the current study, the value for R_s was computed by using methods developed by Cheung. The equation by means of Cheung's method can be expressed as [18, 23, 28, 29]

$$\frac{dV}{d(\ln J)} = AR_sJ + \frac{nkT}{q}, \tag{5}$$

$$H(J) = AR_sJ + n\phi_b = V - \frac{nkT}{q}\ln\left(\frac{J}{A^*T^2}\right), \tag{6}$$

where R_s, ϕ_b, A^*, and A are series resistance, barrier height, Richardson's constant of β-$FeSi_2$, and area of heterojunctions, respectively.

Based on (5), the relationship of $dV/d(\ln J)$-J was plotted on the left axis at (a) 300 K and (b) 20 K, as displayed in Figure 6. From this plot, nkT/q and AR_s were computed from the *y*-axis intercept and slope, respectively. In order to affirm agreement of the value for R_s by using (6), $H(J)$-J on the right axis in Figure 6 was also plotted at (a) 300 K and (b) 20 K. The values for AR_s and $n\phi_b$ were computed from the slope and intercept point of the *y*-axis, respectively. From the computations, the *n* values were 1.63 at 300 K and 16.13 at 20 K, while the ϕ_b values were 0.54 eV at 300 K and 0.05 eV at 20 K. These values agreed with those computed from the TE theory. More importantly, the R_s values computed from the relationship of $dV/d(\ln J)$-J were 13.05 Ω at 300 K and 0.14 MΩ at 20 K. From the $H(J)$-J plot, the R_s values were 13.18 Ω at 300 K and 0.14 MΩ at 20 K. These results proved that the R_s values computed from the relationship of $dV/d(\ln J)$-J were approximately equal to those computed from the relationship of $H(J)$-J. The increasing R_s values at low temperatures were likely due to the increment of *n* value at low temperatures.

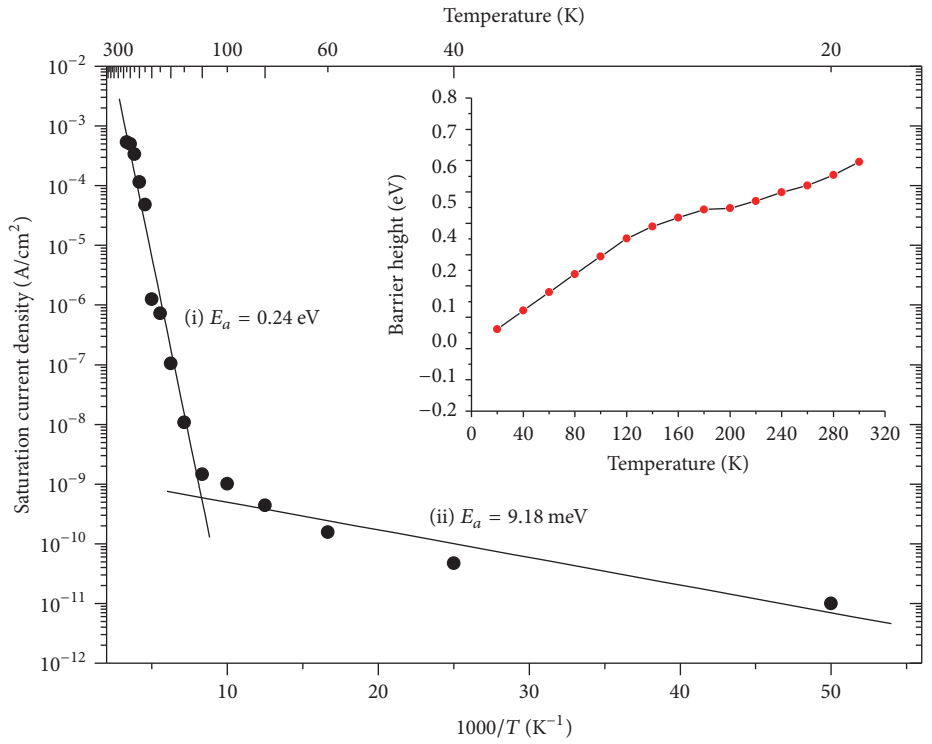

Figure 5: Arrhenius plot for log J_0 versus 1000/T. The inset is a plot of the ϕ_b value versus temperature.

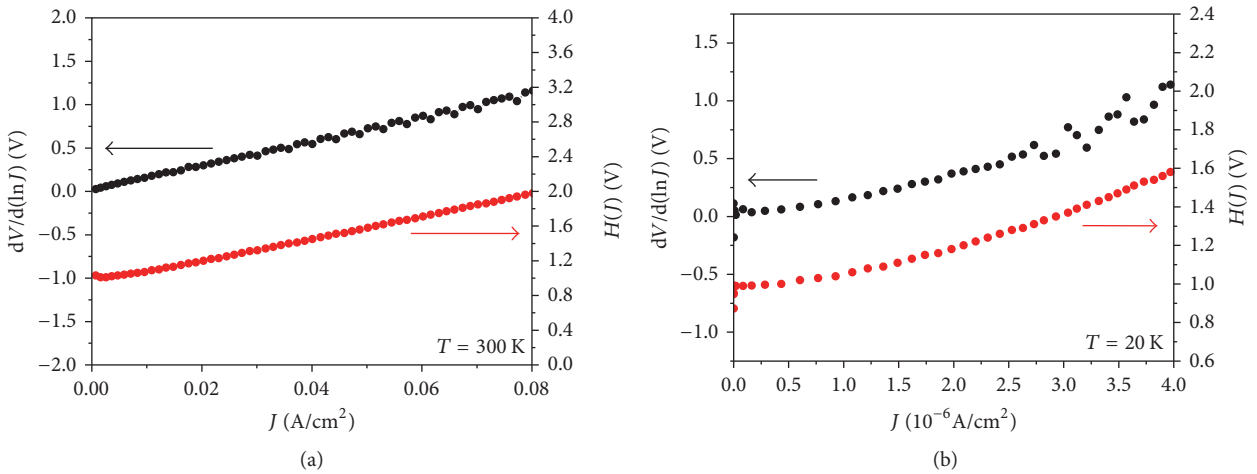

Figure 6: Relationship between dV/d(ln J)-J (left axis) and $H(J)$-J (right axis) at temperatures of (a) 300 K and (b) 20 K.

Besides, the current study utilized Norde's method to compute the R_s value. The relationship based on Norde's method can be derived as [19, 30]

$$F(V) = \frac{V}{\gamma} - \frac{kT}{q} \ln\left(\frac{J}{A^* T^2}\right), \tag{7}$$

where V is bias voltage, J is the voltage-dependent forward current density, T is temperature, and γ is the first integer higher than the n value. Both the ϕ_b and R_s values could be computed by determining the minimum of $F(V)$-V in the following equation:

$$\phi_b = F(V_0) + \frac{V_0}{\gamma} - \frac{kT}{q}, \tag{8}$$

where $F(V_0)$ is the minimum of $F(V)$ and V_0 is the corresponding voltage, and

$$R_s = (\gamma - n)\frac{kT}{qJ_{\min}A}, \tag{9}$$

where A is the area of the heterojunctions and $J_{\min}$ is the corresponding current density.

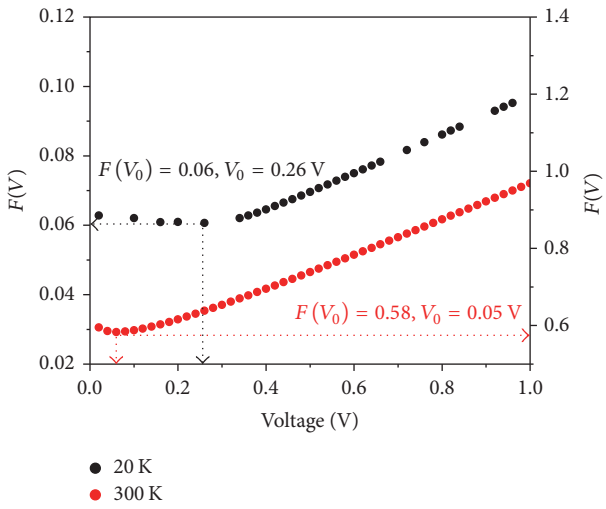

FIGURE 7: Plots of $F(V)$-V at 20 K (left axis) and at 300 K (right axis).

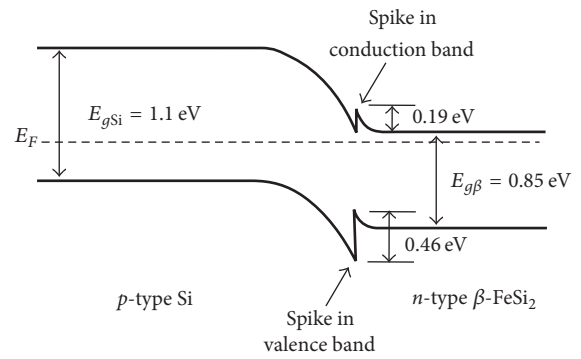

FIGURE 8: Energy band diagram that indicates the spikes in conduction and valence bands for n-type β-$FeSi_2$/p-type Si heterojunctions.

The plots of $F(V)$-V at temperatures of 300 K (red line) and 20 K (black line) are displayed in Figure 7. From the plot at 300 K, the values for $F(V_0)$ and V_0 were 0.58 and 0.05 V, respectively. The values for $F(V_0)$ and V_0 at 20 K changed to 0.06 and 0.26 V, respectively. Based on the computation using (8), the ϕ_b values were 0.58 eV at 300 K and 0.07 eV at 20 K. In addition, R_s value computed by (9) was 10.93 Ω at 300 K and enhanced dramatically to 0.15 MΩ at 20 K. The results from computation using Norde's method were in agreement with those computed by the TE theory and Cheung's method.

The NIR light detection for n-type β-$FeSi_2$/p-type Si heterojunctions formed by RFMS was experimentally demonstrated in a previous study [15]. Their light detection performance was unexpectedly degraded. In order to understand the causes of this degradation, junction parameters such as n and R_s were investigated in the current study. At room temperature, the junctions revealed a large reverse leakage current together with a weak response for NIR light irradiation [15]. From the computation of the junction parameters, the n value was found to be >1 and ≤2 at room temperature. The implication is that the carrier recombination process was dominant in the transportation mechanism across the heterojunction interface [31]. The presence of defects in β-$FeSi_2$ thin films might generate deep energy levels in the bandgap, which could behave as recombination centers [31]. For this reason, the weak response of NIR light was likely due to the recombination of photocarriers at the heterojunction interface, resulting from the presence of defects [32]. Additionally, the estimated R_s value, which was 13.05 Ω at room temperature, might be attributed to the diffusion of Fe atoms into the Si side [33]. The diffused Fe atoms generate deep trap levels in the depletion region, which produce the leakage current in the formed heterojunctions [33, 34]. Moreover, the NIR light detection was spoiled because the photogenerated carriers were trapped in the deep trap levels owing to the diffusion of Fe atoms [33, 34].

At low temperatures, the ratio between the photocurrent and dark current was increased, which was probably due to the reduction of the reverse leakage current at low temperatures [15]. This reduction of leakage current is attributable to the decreased carrier densities in the β-$FeSi_2$ films at low temperatures [15, 31, 35]. Unexpectedly, the photocurrent decreased along with the decrease of the leakage current at low temperatures [15]. Based on the computation of the n value, this value increased to be >2 at low temperatures. This might imply that a tunneling process contributed to the carrier transportation mechanism [31]. This is likely owing to the existence of interface states at the heterojunction interface [31]. The existent interface states could behave as a trap center of photogenerated carriers [35], which would be the possible cause for the reduction of photocurrent at low temperatures. Additionally, we consider that the carrier tunneling process implies the appearance of spikes in conduction and valence bands owing to a heterojunction band offset as shown in Figure 8. These spikes prevent the flow of photogenerated carriers at the heterojunction interface. The decreased photocurrent at low temperatures might be because the spikes that appear in conduction and valence bands are higher at low temperatures and they could behave as a barrier for the photogenerated carriers flowing at the heterojunction interface. It is expected that the spikes were enlarged at low temperatures owing to the Fermi levels of Si and β-$FeSi_2$ layers approaching the center of the band gaps at low temperatures. Also, from the computation of the R_s, this parameter increased at low temperatures. This might be attributable to the low mobility of carriers in the β-$FeSi_2$ thin films, which degrades at low temperatures [36].

4. Conclusions

Measurement and analysis were conducted on n-type β-$FeSi_2$/p-type Si heterojunctions grown by RFMS for the dark J-V curves as a function of temperature. Their heterojunction parameters were systematically computed using the TE theory, Cheung's method, and Norde's method. From computation using the TE theory, the value of n was 1.71 at 300 K and increased to 16.83 at 20 K, whereas the ϕ_b value was 0.59 eV at 300 K and decreased to 0.06 eV at 20 K. The values for both n and ϕ_b were approximately equal to those computed from Cheung's and Norde's methods. The values

for R_s computed by Cheung's method were 13.05 Ω at 300 K and 0.14 MΩ at 20 K, which were approximately equal to those computed using Norde's method.

Competing Interests

The authors declare that they have no competing interests.

Acknowledgments

This work was supported financially by a research fund from AUN/SEED-Net in the Collaborative Research Program for Alumni Members (CRA) Project and King Mongkut's Institute of Technology Ladkrabang.

References

[1] T. Sunohara, K. Kobayashi, and T. Suemasu, "Epitaxial growth and characterization of Si-based light-emitting Si/β-$FeSi_2$ film/Si double heterostructures on Si(001) substrates by molecular beam epitaxy," *Thin Solid Films*, vol. 508, no. 1-2, pp. 371–375, 2006.

[2] D. Leong, M. Harry, K. J. Reeson, and K. P. Homewood, "A silicon/iron-disilicide light-emitting diode operating at a wavelength of 1.5 μm," *Nature*, vol. 387, no. 6634, pp. 686–688, 1997.

[3] T. Suemasu, Y. Ugajin, S. Murase, T. Sunohara, and M. Suzuno, "Photoluminescence decay time and electroluminescence of p-Si/β-$FeSi_2$ particles/n-Si and p-Si/β-$FeSi_2$ film/n-Si double-heterostructures light-emitting diodes grown by molecular-beam epitaxy," *Journal of Applied Physics*, vol. 101, no. 12, Article ID 124506, 2007.

[4] B. Tatar, K. Kutlu, and M. Ürgen, "Synthesis of β-$FeSi_2$/Si heterojunctions for photovoltaic applications by unbalanced magnetron sputtering," *Thin Solid Films*, vol. 516, no. 1, pp. 13–16, 2007.

[5] M. Z. Hossain, T. Mimura, N. Miura, and S.-I. Uekusa, "Surface morphology and luminescence characterization of β-$FeSi_2$ thin films prepared by pulsed laser deposition," *Applied Surface Science*, vol. 256, no. 4, pp. 1227–1231, 2009.

[6] M. C. Bost and J. E. Mahan, "A clarification of the index of refraction of beta-iron disilicide," *Journal of Applied Physics*, vol. 64, no. 4, pp. 2034–2037, 1988.

[7] N. Promros, K. Yamashita, R. Iwasaki, and T. Yoshitake, "Effects of hydrogen passivation on near-infrared photodetection of n-type β-$FeSi_2$/p-type Si heterojunction photodiodes," *Japanese Journal of Applied Physics*, vol. 51, no. 10R, Article ID 108006, 2012.

[8] N. Promros, K. Yamashita, S. Izumi, R. Iwasaki, M. Shaban, and T. Yoshitake, "Near-infrared photodetection of n-type β-$FeSi_2$/intrinsic Si/p-type Si heterojunctions at low temperatures," *Japanese Journal of Applied Physics*, vol. 51, no. 9S2, Article ID 09MF02, 2012.

[9] M. Milosavljević, L. Wong, M. Lourenço et al., "Correlation of structural and optical properties of sputtered $FeSi_2$ thin films," *Japanese Journal of Applied Physics*, vol. 49, no. 8, Article ID 081401, 2010.

[10] J. E. Mahan, K. M. Geib, G. Y. Robinson et al., "Epitaxial films of semiconducting $FeSi_2$ on (001) silicon," *Applied Physics Letters*, vol. 56, no. 21, pp. 2126–2128, 1990.

[11] Z. Yang and K. P. Homewood, "Effect of annealing temperature on optical and structural properties of ion-beam-synthesized semiconducting $FeSi_2$ layers," *Journal of Applied Physics*, vol. 79, no. 8, pp. 4312–4317, 1996.

[12] M. Tanaka, Y. Kumagai, T. Suemasu, and F. Hasegawa, "Reactive deposition epitaxial growth of β-$FeSi_2$ layers on Si(001)," *Applied Surface Science*, vol. 117-118, pp. 303–307, 1997.

[13] M. Shaban, K. Nomoto, K. Nakashima, and T. Yoshitake, "Low-temperature annealing of n-type β-$FeSi_2$/p-type Si heterojunctions," *Japanese Journal of Applied Physics*, vol. 47, no. 5, pp. 3444–3446, 2008.

[14] K. Wunstel and P. Wagner, "Interstitial iron and iron-acceptor pairs in silicon," *Applied Physics A Solids and Surfaces*, vol. 27, no. 4, pp. 207–212, 1982.

[15] N. Promros, R. Baba, M. Takahara et al., "Epitaxial growth of β-$FeSi_2$ thin films on Si(111) substrates by radio frequency magnetron sputtering and their application to near-infrared photodetection," *Japanese Journal of Applied Physics*, vol. 55, no. 6S2, Article ID 06HC03, 2016.

[16] D. A. Aldemir, M. Esen, A. Kökce, S. Karataş, and A. F. Özdemir, "Analysis of current–voltage and capacitance–voltage-frequency characteristics in Al/p-Si Schottky diode with the polythiophene-SiO_2 nanocomposite interfacial layer," *Thin Solid Films*, vol. 519, no. 18, pp. 6004–6009, 2011.

[17] S. Duman, B. Gürbulak, S. Doğan, and A. Türüt, "Electrical characteristics and inhomogeneous barrier analysis of Au–Be/p-InSe:Cd Schottky barrier diodes," *Microelectronic Engineering*, vol. 86, no. 1, pp. 106–110, 2009.

[18] S. K. Cheung and N. W. Cheung, "Extraction of Schottky diode parameters from forward current–voltage characteristics," *Applied Physics Letters*, vol. 49, no. 2, pp. 85–87, 1986.

[19] H. Norde, "A modified forward I–V plot for Schottky diodes with high series resistance," *Journal of Applied Physics*, vol. 50, no. 7, pp. 5052–5053, 1979.

[20] S. Sönmezoğlu, "Current transport mechanism of n-TiO_2/p-ZnO heterojunction diode," *Applied Physics Express*, vol. 4, no. 10, Article ID 104104, 2011.

[21] F. Ö. Kuş, T. Serin, and N. Serin, "Current transport mechanisms of n-ZnO/p-CuO heterojunctions," *Journal of Optoelectronics and Advanced Materials*, vol. 11, no. 11, pp. 1855–1859, 2009.

[22] A. A. Farag, I. S. Yahia, T. Wojtowicz, and G. Karczewski, "Influence of temperature and illumination on the electrical properties of p-ZnTe/n-CdTe heterojunction grown by molecular beam epitaxy," *Journal of Physics D: Applied Physics*, vol. 43, no. 21, Article ID 215102, 2010.

[23] H. S. Hafez, I. S. Yahia, G. B. Sakr, M. S. A. Abdel-Mottaleb, and F. Yakuphanoglu, "Extraction of the DSC parameters based titanium under dark and illumination condition," *Advances in Materials and Corrosion*, vol. 1, no. 1, pp. 8–13, 2012.

[24] D. Song and B. Guo, "Electrical properties and carrier transport mechanisms of n-ZnO/SiO_x/n-Si isotype heterojunctions with native or thermal oxide interlayers," *Journal of Physics D: Applied Physics*, vol. 42, no. 2, Article ID 025103, 2009.

[25] M. Caglar and F. Yakuphanoglu, "Fabrication and electrical characterization of flower-like CdO/p-Si heterojunction diode," *Journal of Physics D: Applied Physics*, vol. 42, no. 4, Article ID 045102, 2009.

[26] T. Serin, S. Gürakar, N. Serin, N. Yıldırım, and F. Özyurt Kuş, "Current flow mechanism in Cu_2O/p-Si heterojunction prepared by chemical method," *Journal of Physics D: Applied Physics*, vol. 42, no. 22, Article ID 225108, 2009.

[27] Y. P. Song, R. L. Van Meirhaeghe, W. H. Laflère, and F. Cardon, "On the difference in apparent barrier height as obtained from

capacitance-voltage and current-voltage-temperature measurements on Al/*p*-InP Schottky barriers," *Solid State Electronics*, vol. 29, no. 6, pp. 633–638, 1986.

[28] A. M. Rodrigues, "Extraction of Schottky diode parameters from current-voltage data for a chemical-vapor-deposited diamond/silicon structure over a wide temperature range," *Journal of Applied Physics*, vol. 103, no. 8, Article ID 083708, 2008.

[29] O. F. Yuksel, "Temperature dependence of current-voltage characteristics of Al/p-Si (1 0 0) Schottky barrier diodes," *Physica B*, vol. 404, no. 14-15, pp. 1993–1997, 2009.

[30] S. Baturay, Y. S. Ocak, and D. Kaya, "The effect of Gd doping on the electrical and photoelectrical properties of Gd:ZnO/p-Si heterojunctions," *Journal of Alloys and Compounds*, vol. 645, pp. 29–33, 2015.

[31] N. Promros, R. Baba, H. Kishimoto et al., "Characterization of n-type nanocrystalline iron disilicide/intrinsic ultrananocrystalline diamond/amorphous carbon composite/p-type silicon heterojunctions at low temperatures," *Journal of Nanoelectronics and Optoelectronics*, vol. 11, no. 5, pp. 579–584, 2016.

[32] M. Shaban, K. Kawai, N. Promros, and T. Yoshitake, "n-Type nanocrystalline-$FeSi_2$/p-type Si heterojunction photodiodes prepared at room temperature," *IEEE Electron Device Letters*, vol. 31, no. 12, pp. 1428–1430, 2010.

[33] M. Shaban, S. Izumi, K. Nomoto, and T. Yoshitake, "n-Type β-$FeSi_2$/intrinsic-Si/p-type Si heterojunction photodiodes for near-infrared light detection at room temperature," *Applied Physics Letters*, vol. 95, no. 16, Article ID 162102, 2009.

[34] S. Izumi, M. Shaban, N. Promros, K. Nomoto, and T. Yoshitake, "Near-infrared photodetection of β-$FeSi_2$/Si heterojunction photodiodes at low temperatures," *Applied Physics Letters*, vol. 102, no. 3, Article ID 032107, 2013.

[35] N. Promros, K. Yamashita, C. Li et al., "n-Type nanocrystalline $FeSi_2$/intrinsic Si/p-type Si heterojunction photodiodes fabricated by facing-target direct-current sputtering," *Japanese Journal of Applied Physics*, vol. 51, no. 2R, Article ID 021301, 2012.

[36] A. Zkria, M. Shaban, T. Hanada, N. Promros, and T. Yoshitake, "Current transport mechanisms in *n*-type ultrananocrystalline diamond/p-type Si heterojunctions," *Journal of Nanoscience and Nanotechnology*, vol. 16, no. 12, pp. 12749–12753, 2016.